**The EMBO Journal (2011) 30,** 3799–3811 | © 2011 European Molecular Biology Organization | All Rights Reserved 0261-4189/11
www.embojournal.org

THE EMBO JOURNAL

# Ribosome biogenesis factors bind a nuclear envelope SUN domain protein to cluster yeast telomeres

**Chihiro Horigome[1,2], Takafumi Okada[1], Kyoko Shimazu[1], Susan M Gasser[2] and Keiko Mizuta[1,*]**

[1]Department of Biofunctional Science and Technology, Graduate School of Biosphere Science, Hiroshima University, Higashi-Hiroshima, Japan and [2]Friedrich Miescher Institute for Biomedical Research, Basel, Switzerland

**Two interacting ribosome biogenesis factors, Ebp2 and Rrs1, associate with Mps3, an essential inner nuclear membrane protein. Both are found in foci along the nuclear periphery, like Mps3, as well as in the nucleolus. Temperature-sensitive *ebp2* and *rrs1* mutations that compromise ribosome biogenesis displace the mutant proteins from the nuclear rim and lead to a distorted nuclear shape. Mps3 is known to contribute to the S-phase anchoring of telomeres through its interaction with the silent information regulator Sir4 and yKu. Intriguingly, we find that both Ebp2 and Rrs1 interact with the C-terminal domain of Sir4, and that conditional inactivation of either *ebp2* or *rrs1* interferes with both the clustering and silencing of yeast telomeres, while telomere tethering to the nuclear periphery remains intact. Importantly, expression of an Ebp2–Mps3 fusion protein in the *ebp2* mutant suppresses the defect in telomere clustering, but not its defects in growth or ribosome biogenesis. Our results suggest that the ribosome biogenesis factors Ebp2 and Rrs1 cooperate with Mps3 to mediate telomere clustering, but not telomere tethering, by binding Sir4.**

*The EMBO Journal* (2011) **30,** 3799–3811. doi:10.1038/emboj.2011.267; Published online 5 August 2011
*Subject Categories*: chromatin & transcription; proteins
*Keywords*: nuclear envelope; ribosome biogenesis; SUN protein; telomere clusters; telomeric silencing

## Introduction

All protein synthesis depends on the ribosome, a huge RNA–protein complex containing four different ribosomal RNAs (rRNAs; 25S/28S, 18S, 5.8S and 5S rRNA) and about 80 ribosomal proteins. In yeast, all rRNAs are generated as a single precursor synthesized by RNA polymerase I, except the 5S rRNA, which is transcribed by RNA polymerase III. Early 90S pre-ribosome particles are formed in the nucleolus by recruitment of both ribosomal and non-ribosomal proteins onto the transcript. The multistep maturation process occurs sequentially in the nucleolus, the nucleoplasm and the cytoplasm, where pre-ribosome particles are converted to functional 40S and 60S ribosome subunits (reviewed by Tschochner and Hurt, 2003).

In rapidly proliferating eukaryotic cells, ribosome production consumes an enormous fraction of the cell's resources. To cope with this, cells must tightly regulate ribosome biogenesis (reviewed by Warner, 1999 and Moss, 2004). A combination of TAP purification and proteome analysis has revealed that around 200 non-ribosomal proteins are required for pre-rRNA processing and assembly of the 60S and 40S subunits in *Saccharomyces cerevisiae* (reviewed by Henras *et al*, 2008). Many homologues of these regulatory or assembly proteins have been identified in the nucleolar fraction that was isolated from human cells (Andersen *et al*, 2002; Scherl *et al*, 2002), suggesting that mechanisms that produce ribosomes are conserved among eukaryotes. Recent studies have shown that some *bona fide* ribosome synthesis factors function in a range of other cellular processes in yeast, extending well beyond ribosome biogenesis (reviewed by Dez and Tollervey, 2004). However, it remains unclear how ribosome synthesis itself is coordinated with other cellular mechanisms.

We have previously shown that Rrs1 and its interacting protein Ebp2 are required for the maturation of 25S rRNA and the production of the 60S ribosomal subunit in yeast (Tsujii *et al*, 2000; Tsuno *et al*, 2000). In this study, we show that Ebp2 and Rrs1 associate with Mps3, an essential inner nuclear membrane protein, and that both are localized to the nuclear periphery as well as to the nucleolus. Mps3 belongs to the SUN (for *S*ad1-*UN*C84 homology) protein family (Jaspersen *et al*, 2006) which is found in all eukaryotes. In many species, SUN domain proteins have a structural role by bridging from the cytoskeleton through the nuclear envelope to the nuclear interior (Crisp *et al*, 2006), where they affect a range of cellular functions (reviewed by Tzur *et al*, 2006). Mps3, the only SUN protein in budding yeast, is involved in spindle pole body (SPB) duplication in mitotic cells and telomere anchoring at the nuclear periphery in both mitotic and meiotic cells (Jaspersen *et al*, 2002; Nishikawa *et al*, 2003; Antoniacci *et al*, 2007; Bupp *et al*, 2007; Conrad *et al*, 2007, 2008; Schober *et al*, 2009).

In mitosis, yeast telomeres are anchored in clusters at the nuclear periphery through two partially redundant pathways, the Sir4- and yeast Ku- (yKu; Yku70/Yku80 heterodimer) anchorage pathway (Hediger *et al*, 2002; Taddei *et al*, 2004). In both cases, these telomere-associated factors bind nuclear envelope proteins to establish a specialized subnuclear compartment, in which telomeres are sequestered. One pathway tethers SIR-repressed chromatin through the interaction of the Sir4 PAD domain with Esc1, a peripheral membrane anchor (Hediger *et al*, 2002; Taddei *et al*, 2004;

*Corresponding author. Department of Biofunctional Science and Technology, Graduate School of Biosphere Science, Hiroshima University, 1-4-4 Kagamiyama, Higashi-Hiroshima 739-8528, Japan. Tel./Fax: +81 82 424 7923; E-mail: kei7mizuta@hiroshima-u.ac.jp

**Received: 15 January 2010; accepted: 7 July 2011; published online: 5 August 2011**

Bupp *et al*, 2007). This occurs independently of yKu and Mps3. In S-phase cells, on the other hand, the yKu pathway of telomere anchoring requires telomerase RNA, its protein subunits, Est2 and Est1, and interaction with an 80-aa acidic domain in the N-terminus of Mps3 (Antoniacci *et al*, 2007; Schober *et al*, 2009). Deletion of the Mps3 N-terminus specifically compromises telomere anchoring in S-phase cells (Bupp *et al*, 2007; Schober *et al*, 2009). Given that Mps3 also precipitates with Sir4, we conclude that telomere position in mitotic yeast nuclei is maintained through redundant and partially overlapping sets of interactions between membrane-associated and telomere-bound proteins showing tight cell-cycle regulation (Hediger *et al*, 2002; Taddei *et al*, 2004; Ebrahimi and Donaldson, 2008).

Here, we suggest that Ebp2 and Rrs1 contribute to this telomere organization network. We find that Ebp2 and Rrs1 localize to the nuclear envelope as well as to the nucleolus, independently of Sir4. Mutations in *EBP2* and *RRS1* that retard rRNA processing, also affect telomere clustering and subtelomeric silencing, but not anchoring at the nuclear envelope. The telomere and ribosome assembly defects become manifest in the temperature-sensitive strains with very different kinetics. Importantly, we are able to separate the telomere function of Ebp2 from its role in ribosome biogenesis, by expressing it as a fusion to Mps3. This construct localizes to the nuclear envelope and restores the telomere clustering function of Ebp2, but does not suppress the ribosomal defects of the *ebp2* mutant strain. This substantiates the argument that Ebp2 has an independent function in telomere maintenance.

## Results

### *ebp2 and rrs1 conditional mutants lead to nuclear deformation as well as defects in ribosome biogenesis*

By random PCR mutagenesis, we generated several temperature-sensitive *ebp2* and *rrs1* mutants. Each of the mutants has nucleotide changes in regions that are highly conserved from yeast to human (Miyoshi *et al*, 2004; Horigome *et al*, 2008). [*Methyl*-$^{3}$H] methionine pulse-chase and polysome analyses revealed that 25S rRNA maturation and 60S ribosomal subunit production are compromised in temperature-sensitive *ebp2* and *rrs1* mutants grown at the restrictive temperature (Figure 1A and B; Miyoshi *et al*, 2004; Horigome *et al*, 2008), indicating that Ebp2 and Rrs1 indeed regulate the rate of ribosome biogenesis. We used *ebp2-14* and *rrs1-124* for further analyses, because temperature sensitivity of *ebp2-7* was very weak, *ebp2-12* exhibited slight defects in growth and ribosome biogenesis even at 25°C (Horigome *et al*, 2008), and *rrs1-84* caused reduction of cellular concentration of the mutant form of Rrs1 at the restrictive temperature (Miyoshi *et al*, 2004).

Intriguingly, coincident with impaired 60S ribosomal subunit biogenesis, we found a striking morphological phenotype in the nuclei of the *ebp2-14* and *rrs1-124*. Immunofluorescence microscopy with antibodies against nuclear pore complex (NPC) proteins showed that the nuclear envelope in mutant cells became distorted into a non-spherical shape at the restrictive temperature, but not at the permissive temperature (see arrows in Figure 2A). This is not due to a disruption of nucleolar structure, which is closely tied to ribosome biogenesis, because Nop1, a well-known nucleolar protein that has a role in rRNA methylation, showed an intact nucleolar structure in *ebp2-14* and *rrs1-124* mutants at 37 °C (see YFP–Nop1; Supplementary Figure S1A). We, therefore, further explored the possibility that Ebp2 and Rrs1 have a distinct role in the maintenance of nuclear organization, in addition to their role in ribosome biogenesis.

### *Ebp2 and Rrs1 are localized not only to the nucleolus but also to the nuclear periphery*

To examine whether Ebp2 and Rrs1 might function at the nuclear envelope, we analysed the subnuclear localization of these proteins in detail. We constructed strains expressing Ebp2 or Rrs1 fused to enhanced green fluorescent protein (EGFP) at their endogenous loci, expressed from their own promoters. The fusions had little effect on growth rate of wild type (data not shown). Surprisingly, EGFP–Ebp2 and EGFP–Rrs1 fusions generated punctate signals at the nuclear periphery as well as labelling the crescent-shaped nucleolus. The signals remain associated with the nuclear envelope through mitosis (Figure 2B).

We confirmed the localization of Ebp2 and Rrs1 by indirect immunofluorescence microscopy. We acquired 8-step image stacks and analysed them with constrained iterative (CI) deconvolution, which confirmed the punctate distribution of Ebp2 and Myc-tagged Rrs1 at the nuclear periphery (Supplementary Figure S1B and C). A typical nucleolar marker like Nop1, on the other hand, was not observed at the nuclear periphery. Quantification of fluorescence intensity by line scanning across a nuclear plane reveals the bimodal distribution of Ebp2, which unlike Nop1 is both at the nuclear periphery and in the nucleolus (Supplementary Figure S1D).

Double staining showed that Ebp2 colocalizes precisely with Rrs1–9Myc at the nuclear periphery (Supplementary Figure S1C). On the other hand, in the nucleolar compartment, both proteins appear to surround the rDNA, but Rrs1–9Myc generally had a more peripheral distribution than Ebp2. This suggests that despite their ability to interact (see below) the two proteins may not always form a heterodimer (Supplementary Figure S1C).

### *Mutant forms of Ebp2 and Rrs1 lose association with the nuclear periphery*

We next examined whether the *ebp2-14* and *rrs1-124* alleles that lead to nuclear deformation also affect the subnuclear distribution of the mutant proteins. We generated strains expressing wild-type or mutant forms of Ebp2 fused EGFP, or else wild-type or mutant forms of Rrs1 fused to cyan fluorescent protein (CFP). *EGFP-ebp2-14* and *CFP-rrs1-124* mutants exhibited a fluorescent signal at the nuclear periphery at permissive temperature, which was lost when cells were placed at 37°C (Figure 2C). Although the *ebp2-14* and *rrs1-124* strains have deformed nuclei at the restrictive temperature (Figure 2A), the EGFP–ebp2-14 and CFP–rrs1-124 signals in the nucleolus were not affected by the temperature shift (Figure 2C). Thus, we observed a correlation between the punctate perinuclear localization of both Ebp2 and Rrs1, and maintenance of a spherical nuclear shape. In Figure 2C, the nucleolar signal of CFP–rrs1-124 is also more diffuse than the corresponding wild-type protein, whereas YFP–Nop1 shows an intact nucleolar structure at 37°C (Supplementary Figure S1A).

 

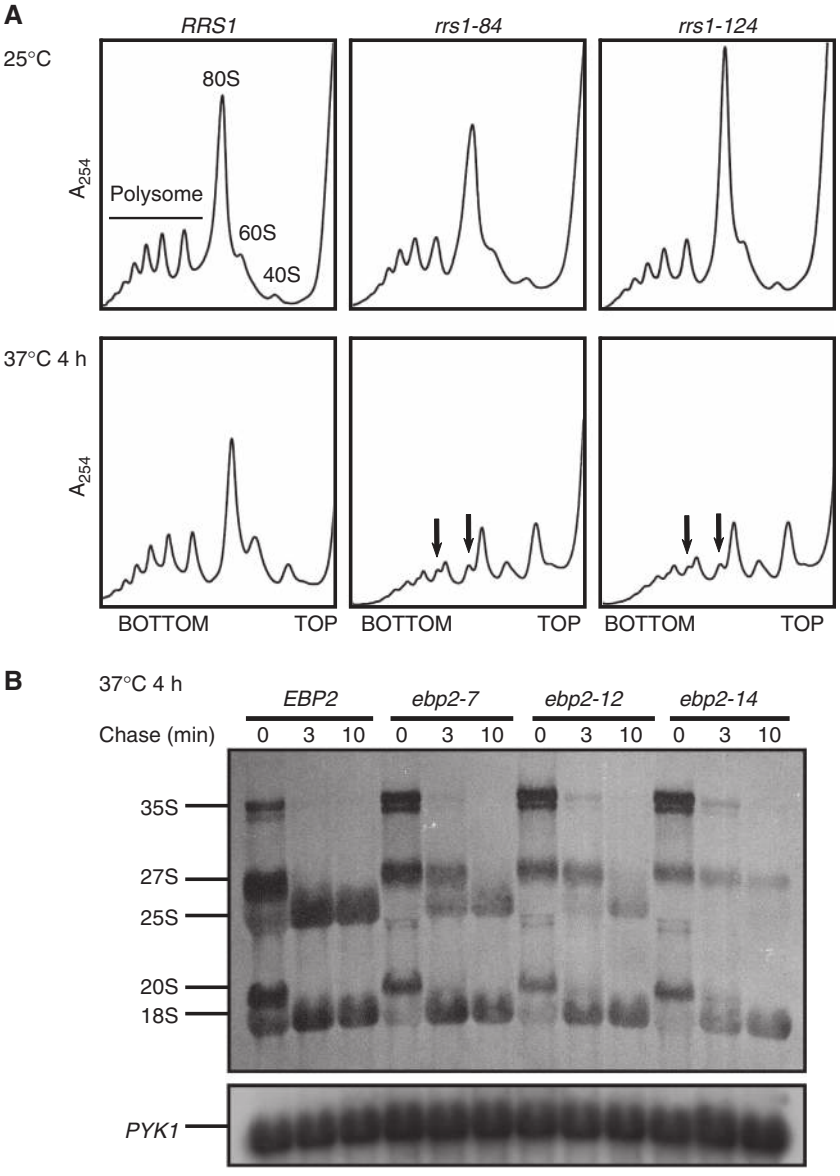


**Figure 1** The *ebp2* and *rrs1* mutants are defective in 60S ribosomal subunit biogenesis. (**A**) Polysome profiles in *rrs1* mutants. *RRS1* (KM370) and *rrs1* (*rrs1-84*: KM921, *rrs1-124*: KM923) cells cultured at 37°C for 4 h were disrupted, and free ribosomal subunits and polysomes in cell extracts were separated. Arrows indicate half-mer polysomes. (**B**) [*Methyl*-$^3$H] methionine pulse-chase analysis of rRNA synthesis in *ebp2* mutant cells. *EBP2* (KM411) and *ebp2* (*ebp2-7*: KM412, *ebp2-12*: KM413, *ebp2-14*: KM414) cells cultured at 37°C for 4 h, pulsed with [*methyl*-$^3$H] methionine, and chased with non-radioactive methionine. Total RNA prepared from each sample was analysed by electrophoresis and blotted onto a membrane. The membrane was sprayed with En$^3$Hance (NEN) and exposed to film. The membrane was reprobed for *PYK1* as a loading marker. [*Methyl*-$^3$H] methionine pulse-chase analysis of rRNA synthesis in *rrs1* mutant cells and polysome profiles in *ebp2* mutants have been reported (Miyoshi *et al*, 2004; Horigome *et al*, 2008).

To understand the kinetics of delocalization, we scored the position of EGFP–ebp2-14 and CFP–rrs1-124 as early as 30 min after the temperature shift. Both proteins became rapidly dispersed from the nuclear periphery (Figure 2C). To see if this correlates with defective ribosome synthesis, we scored this over the same time period. However, little or no defect in ribosome synthesis was observed by 30 min after the temperature shift in either *ebp2-14* or *rrs1-124* cells (Supplementary Figure S2). We conclude that the delocalization of Ebp2 and Rrs1 from the nuclear periphery in the mutant cells is not a secondary effect of impaired ribosome synthesis.

### *Ebp2 and Rrs1 interact with Mps3, a nuclear envelope SUN protein*

An earlier yeast two-hybrid screen for *Schizosaccharomyces pombe* SUN protein Sad1, identified the *Schizosaccharomyces pombe* Ebp2 and Rrs1, as well as 23 other proteins located at the SPB, NPC and nuclear membrane, as ligands of Sad1 (Miki *et al*, 2004). Given that Sad1 spans the inner nuclear membrane, we examined whether the Sad1 orthologue in *S. cerevisiae*, Mps3, might control Ebp2 and Rrs1 positioning at the nuclear periphery.

We first performed *in vitro* pull-down, immunoprecipitation and yeast two-hybrid assays to see if Ebp2 and Rrs1

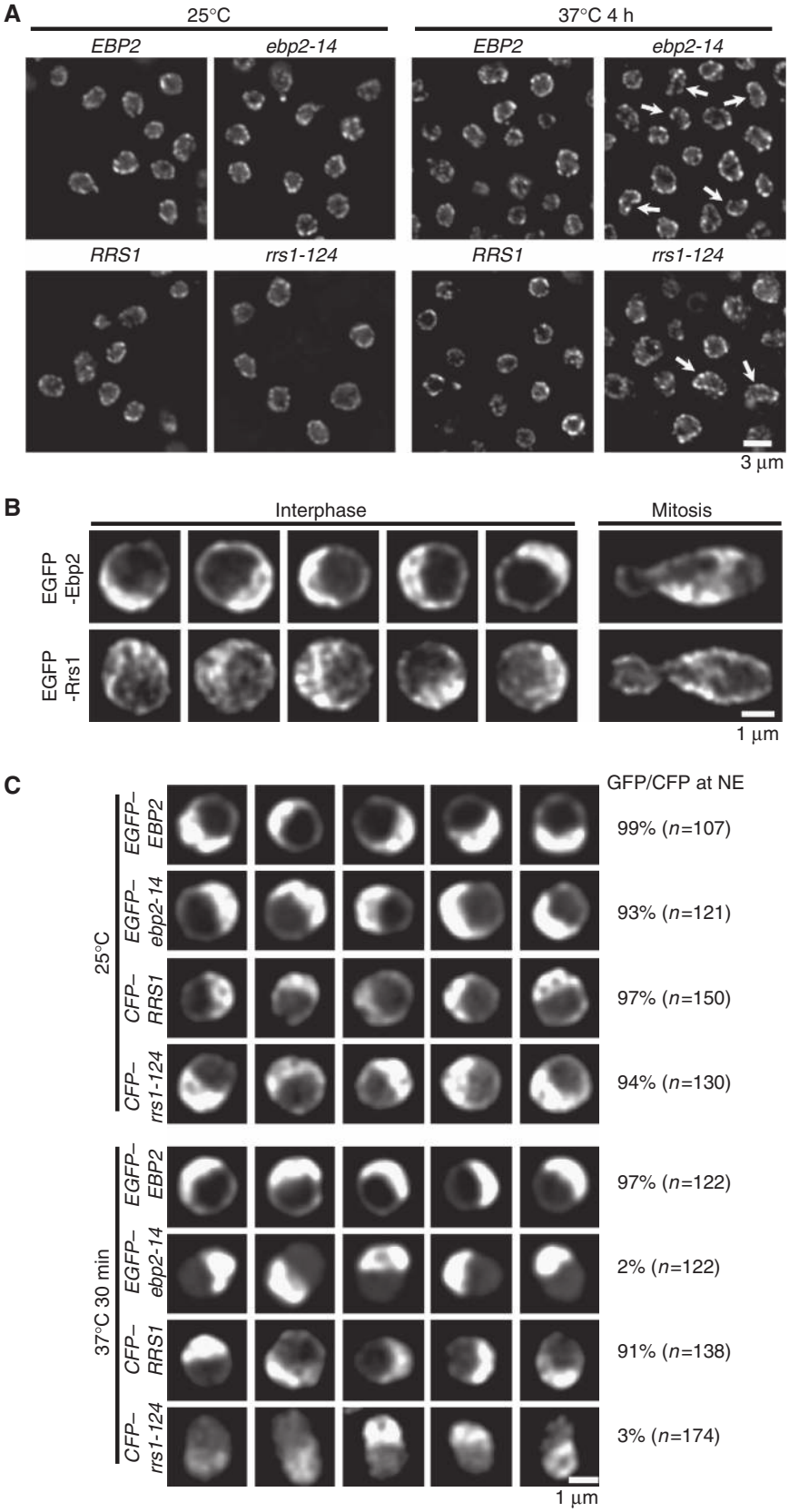


**Figure 2** Ebp2 and Rrs1 are localized to the nuclear periphery and the *ebp2-14* and *rrs1-124* mutations affect the localization to the nuclear periphery. (**A**) Localization of NPC (anti-NPC; white) was observed in wild-type (*EBP2*: KM411, *RRS1*: KM370) and *ebp2-14* (KM414), *rrs1-124* (KM923) mutant cells at 25°C and the restrictive temperature (37°C) for 4 h. Arrows indicate nuclei in deformed shape. (**B**) Localization of EGFP–Ebp2 (KM1067) and EGFP–Rrs1 (KM943) was analysed at 30°C. (**C**) Localization of wild-type EGFP–Ebp2 (KM1067), CFP–Rrs1 (KM1110) and their mutant forms (KM1070 and KM1112) was analysed at 25 and 37°C for 30 min. Typical images are shown. The percentage of the cells in which the signals of EGFP/CFP is detected at the nuclear periphery is shown on the right side. The number of nuclei examined in each dataset is indicated (*n*).

 

interact with Mps3. Glutathione S-transferase (GST)-fused Mps3 and maltose binding protein (MBP) fused to either full-length Rrs1 or the C-terminal half of Ebp2 (aa 212–427) were expressed in *Escherichia coli* and affinity purified for *in vitro* pull-down assay. In Supplementary Figure S3A, we show that GST-fused Mps3 binds directly to MBP fusions with either full-length Rrs1 or the C-terminal half of Ebp2, but not to MBP alone. The co-immunoprecipitation results argue that Ebp2 and Rrs1–9Myc interact with 3HA–Mps3 *in vivo*, albeit weakly (Figure 3A). To identify the domain of Mps3 responsible for the interaction, we tested N- and C-terminal fragments of Mps3 (regions protruding into the nucleoplasm and the intermembrane space, respectively; Nishikawa *et al*, 2003) for interaction with Ebp2 and Rrs1. The N-terminal nucleoplasmic region of Mps3, which also is implicated in interaction with Sir4 and Est1 (Antoniacci *et al*, 2007; Bupp *et al*, 2007; Schober *et al*, 2009), was found to interact with both Ebp2 and Rrs1 (Figure 3B). We note that a C-terminal region of Mps3 was also able to bind Rrs1, yet given that this C-terminal domain is not predicted to extend into the nucleoplasm, the significance of this interaction is unknown. Collectively, these results suggest that Ebp2 and Rrs1 can bind Mps3.

Using deconvolution confocal microscopy, we next showed that EGFP–Mps3 is localized to the nuclear envelope in perinuclear foci, which were largely excluded from CFP-tagged nuclear pores, as well as giving an intense signal at SPB (Figure 3C). To examine whether Ebp2 and Rrs1 bind nuclear pores or Mps3 sites along the nuclear membrane, we introduced an N-terminal deletion of Nup133 (*nup133ΔN*;

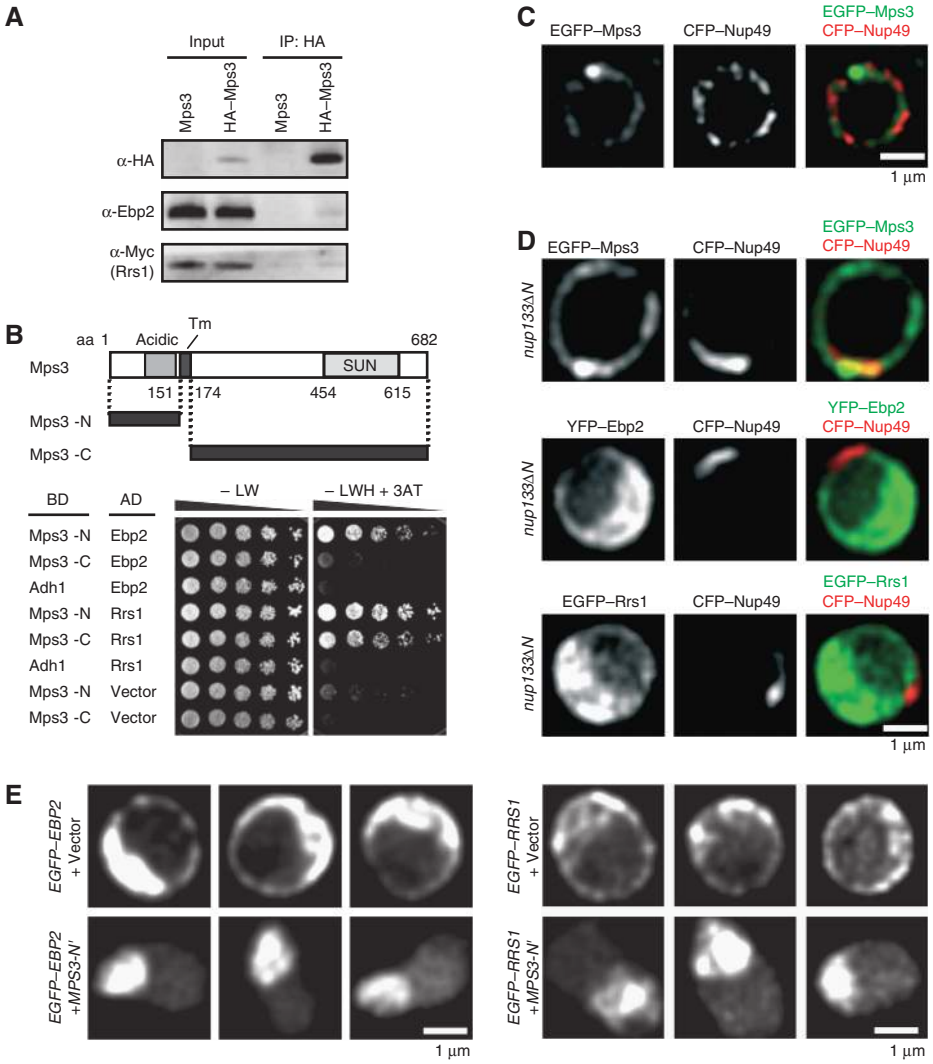


**Figure 3** Ebp2 and Rrs1 interact with a nuclear envelope SUN protein and are localized to non-pore sites along the nuclear envelope. (**A**) Co-immunoprecipitation of Ebp2 and Rrs1–9Myc with 3HA–Mps3. Liquid nitrogen ground lysates were prepared from cells bearing Rrs1–9Myc with 3HA–Mps3 (KM1319) or Mps3 (KM978). The protein composition of lysates and anti-HA immunoprecipitates was analysed by western blotting with anti-HA, anti-Ebp2 and anti-Myc antibodies. (**B**) Two-hybrid interactions of Ebp2 and Rrs1 with Mps3 were detected by the cell growth at 30°C on a medium containing 3-AT at concentration of 0.1 mM. Upper panel shows schematic of Mps3 and its deletion mutants used in two-hybrid analysis. 'Tm' represents a transmembrane domain. (**C**) EGFP–Mps3 and CFP–Nup49 were observed at 30°C (GA6647). (**D**) Localization of EGFP–Mps3 (GA6650), YFP–Ebp2 (GA6648) and EGFP–Rrs1 (GA6651) was compared with that of CFP–Nup49 in NPC clustering cells (*nup133::H nup133ΔN*) at 30°C. (**E**) Localization of EGFP–Ebp2 and EGFP–Rrs1 was monitored by confocal microscopy upon overexpression of the N-terminal domain of Mps3 (aa 1–153; Mps3-N'). *EGFP-EBP2* and *EGFP-RRS1* strains with pRS426-$P_{ADH1}$-*MPS3-N'* (KM1316 and KM1318) or a vector pRS426-$P_{ADH1}$ (KM1315 and KM1317) were cultured at 30°C.

Doye *et al*, 1994) in a strain expressing CFP–Nup49, a subunit of NPC. In the *nup133ΔN* mutant, nuclear pores cluster at one side of the nuclear envelope. However, the distribution of EGFP–Mps3 along the nuclear envelope was unaffected by the clustering of nuclear pores (Figure 3D). Similarly, both YFP–Ebp2 and EGFP–Rrs1 were found at the nuclear periphery, but not together with the clustered CFP pores. We conclude that Epb2 and Rrs1 are localized to the nuclear membrane but are not enriched at pores (Figure 3D). Consistently, Mps3 shows an independent distribution from that of nuclear pores, even though at some positions Mps3 and pore signals coincide. Unlike Mps3, however, YFP–Ebp2 was excluded from the SPB (Supplementary Figure S3B), allowing us to propose that Ebp2 colocalizes with Mps3 along the nuclear membrane, but not at the SPB. Consistently, *ebp2-14* was not synthetic lethal with mutants that compromise spindle checkpoint, in contrast to *mps2-1*, which produces a mutant form of Mps2, a functional partner of Mps3 at the SPB (Supplementary Figure S3C).

To test whether the perinuclear localization of Ebp2 and Rrs1 is dependent on Mps3, we overexpressed the nucleoplasmic N-terminal domain of Mps3 (aa 1–153; Mps3-N') and followed the distribution of EGFP–Ebp2 and EGFP–Rrs1 in its presence. This domain of Mps3 has been shown to have a dominant-negative effect on telomere recombination (Schober *et al*, 2009). Indeed, we found that the ectopic expression of Mps3-N' antagonized the perinuclear localization of both EGFP–Ebp2 and EGFP–Rrs1 (Figure 3E). Intriguingly, the ectopic expression of Mps3-N' also provoked a non-spherical nuclear shape like that seen in *ebp2-14* and *rrs1-124* mutants at restrictive temperature (Figure 2A and C). One interpretation of our data is that Mps3-N', which does not bind the nuclear envelope (Schober *et al*, 2009), titrates Ebp2 and Rrs1 away from their perinulcear binding sites, thereby compromising their role in the maintenance of spherical nuclear shape.

### *Ebp2 and Rrs1 interact with Sir4, the silent information regulator*

Recent advances have shown that proteins of the nuclear envelope help organize chromatin within the nucleus as structural scaffolds (for review, see Towbin *et al*, 2009). To test the hypothesis that Ebp2 and Rrs1 might have implications for telomere organization, we asked whether Ebp2 or Rrs1 interacts with Sir4 using yeast two-hybrid assays. Indeed, Ebp2 and Rrs1 interacted with the C-terminal region of Sir4, namely aa 839–1358, which also contains the residues required for interaction between Sir4 and Mps3 (aa 839–934; Figure 4A; Supplementary Figure S4A; Bupp *et al*, 2007). Both interactions were lost when the Mps3 interaction domain was removed from the Sir4 bait (aa 934–1358; Supplementary Figure S4B). Moreover, the interactions were compromised when the dimerizing coiled-coil domain (aa 1267–1358) was removed from the Sir4 bait, a domain that alone binds Rrs1 but not Ebp2 (Supplementary Figure S4B and C). This suggests that Ebp2 may contact Sir4 through Mps3, while Rrs1 appears able to bind the Sir4 coiled-coil domain independently. However, given that a number of proteins bind the extreme C-terminus of Sir4 (including Rap1, Sir3, yKu70, Ubp3 and Ubp10; Supplementary Figure S4A; Gasser and Cockell, 2001), we cannot rule out the involvement of a bridging partner.

To examine whether the interactions between Ebp2/Rrs1 and Mps3/Sir4 are interdependent, we tested the two-hybrid interactions in mutant strains. The N-terminal region of Mps3 was able to bind Ebp2 and Rrs1 in *sir4*Δ cells, indicating that the both the binding of Ebp2 and of Rrs1 to Mps3 are likely to be direct (Figure 4B). Consistent with this finding, the perinuclear localization of Ebp2 persists in *sir4*Δ cells

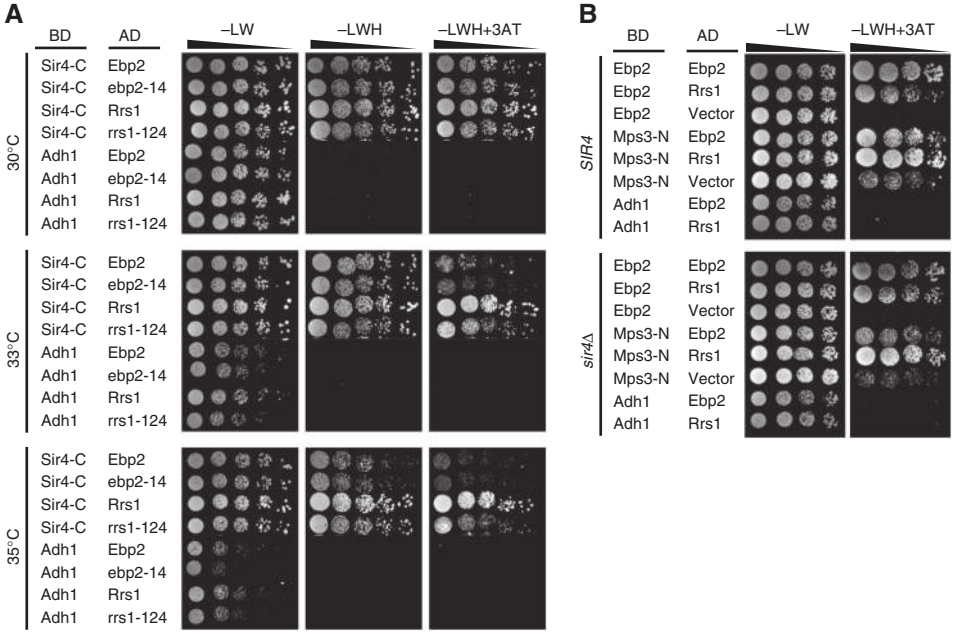


**Figure 4** Ebp2 and Rrs1 interact with Sir4 and the *rrs1-124* mutation affects the interaction. (**A**) Two-hybrid interactions of Ebp2, Rrs1 or their mutant forms with Sir4-C (aa 839–1358) were detected by the cell growth on a medium lacking histidine with or without 0.1 mM 3-AT. (**B**) Interactions among Ebp2, Rrs1 and Mps3 are independent of Sir4. Two-hybrid interactions of Ebp2 with Ebp2 and Rrs1, and Mps3 with Ebp2 and Rrs1 were detected in the *sir4*Δ strain cells (GA6308) grown at 30°C on a medium containing 0.1 mM 3-AT.

 

(Supplementary Figure S5A). Ebp2–Ebp2 and Ebp2–Rrs1 interactions were also independent of the presence of Sir4 (Figure 4B). Interestingly, the *rrs1-124* mutation had a weakened interaction with Sir4 at high temperature, whereas *ebp2-14* at high temperature had little effect on its affinity for Sir4 (Figure 4A). In contrast, neither *rrs1-124* nor *ebp2-14* lost their interactions with the N-terminal region of Mps3 at restrictive temperatures (data not shown). Taken together, we conclude that Rrs1 and Ebp2 can each bind Mps3 independently of Sir4, while the Sir4 C-terminal coiled-coil domain binds Rrs1 but not Ebp2.

### *ebp2 and rrs1 mutations confer defects in telomere clustering and silencing*

Since it has been shown that Mps3 both tethers telomeres at the nuclear periphery and plays a role in their clustering (Antoniacci *et al*, 2007; Bupp *et al*, 2007; Schober *et al*, 2009), we next examined whether Ebp2 and Rrs1 are involved either in the peripheral anchoring or clustering of yeast telomeres in foci. To examine the effect of *ebp2* and *rrs1* mutations on telomere position and clustering, we tagged the telomere repeat binding protein Rap1 (Shore, 1994) by inserting *CFP* into an N-terminal *Nru*I site (Hayashi *et al*, 1998). We carried out 3D live-cell imaging in asynchronously growing cells such that we could score both the number and position of telomeric foci throughout the entire nucleus. In wild-type haploid cells, we found the 32 telomeres clustered in a limited number of perinuclear foci, as previously reported (Gotta *et al*, 1996). By scoring CFP–Rap1 foci in the relevant *ebp2-14* and *rrs1-124* mutants after a shift to 37°C for 30 min, we found more Rap1 foci per nucleus than in the isogenic wild-type cells under similar conditions (Figure 5A). This is reminiscent of the increase in foci number observed in the *mps3Δ65-145* mutant.

It has been demonstrated that yeast telomeres are dynamically rearranged through the cell cycle: telomere clusters dissociate partially in G2/M phase and reform in early G1 (Laroche *et al*, 2000; Hediger *et al*, 2002). The Mps3 N-terminus is required for both yKu- and Sir4-mediated telomere anchoring pathways specifically in S phase (Bupp *et al*, 2007; Schober *et al*, 2009). Therefore, we counted the number of telomere clusters in unbudded (G1 phase) and small-budded (S phase) cells (bud length is $<1/3$ of the mother cell). At permissive temperature, little difference was observed in the cluster number in *ebp2-14* or *rrs1-124* cells compared with that of wild-type cells (Supplementary Figure S6A). However, after 30 min at 37 °C the cluster number in *ebp2-14* and *rrs1-124* S-phase cells increased significantly in the mutant as compared with the wild-type strain (Figure 5B). This was not seen in G1 phase. The *mps3Δ65-145* mutant also had more GFP–Rap1 foci compared with the wild-type strain in S phase (Supplementary Figure S6B). These data suggest that Ebp2 and Rrs1 are required for the maintenance of telomere clusters in S phase, just like their binding partner Mps3.

A recent study has been able to separate the interactions necessary for the peripheral anchoring of *HM* loci from those mediating their interaction in *trans* (Miele *et al*, 2009). Given that Sir4 contributes to both the perinuclear anchoring of silent chromatin at *HM* loci and yeast telomeres (Hediger *et al*, 2002; Gartenberg *et al*, 2004), similar mechanisms are likely to function for both types of loci. However, *trans* interactions at the *HM* loci can be separated from anchoring mechanisms (Miele *et al*, 2009). For this reason, we also scored the position of the telomeric foci relative to the nuclear envelope in *ebp2* and *rrs1* mutants. To calculate the position of the telomere relative to the nuclear periphery, distances between Rap1 foci and nuclear periphery were scored in the plane of focus and were assigned into three zones of equal surface, from the most peripheral zone (1), to the innermost zone (3) (Hediger *et al*, 2002). We find that despite the increase in number at non-permissive temperature in S-phase cells, the positioning of Rap1 foci relative to the nuclear envelope is not altered in the *ebp2-14* or *rrs1-124* strains (Figure 5A and C). This argues that Ebp2 and Rrs1 may contribute to interactions between telomeres in *trans* without disrupting their interaction with the nuclear envelope. This is distinct from the phenotype of *mps3Δ65-145*, which impairs telomere binding to the nuclear envelope as well as telomere clustering (Figure 5A and C).

Proper telomere clustering correlates with telomere silencing (Laroche *et al*, 1998), just as *trans* interactions between *HML* and *HMR* correlate with *HM* repression (Miele *et al*, 2009). Therefore, we next examined whether the *ebp2* and *rrs1* mutations affect the repression of a telomere proximal reporter gene (*URA3*; Figure 5D; Gottschling *et al*, 1990). Indeed, we see a strong disruption of telomeric silencing at 30°C, which is semipermissive temperature in the *ebp2-14* and *rrs1-124* mutants under the experimental conditions, although they were not defective in telomeric silencing at 25°C (Figure 5D). This is not due to an unrelated effect resulting from FOA toxicity combined with the ribosome biogenesis (Hoskins and Butler, 2008), because neither *ebp2-14* nor *rrs1-124* cells exhibit growth defects under the same experimental conditions as the silencing assay at 30°C (Supplementary Figure S7). Collectively, our data suggest that this novel telomere-associated role for Ebp2 and Rrs1 requires interaction with Sir4 and/or Mps3.

### *Ebp2–Mps3 fusion proteins suppress a defect in telomere clustering but not in ribosome biogenesis in the ebp2-14 mutant*

To determine whether the nuclear envelope-bound form of Ebp2 is responsible for telomere clustering, we fused Ebp2 to the N-terminus of Mps3 and tagged them with EGFP. The fusion was expressed under the *MPS3* promoter in the *ebp2-14* mutant cells, to see if it would suppress *ebp2-14* defects. The localization of the resulting EGFP–Ebp2–Mps3 fusion protein was identical to that of endogenous Mps3, that is, at the nuclear membrane and SPB at both 25 and 37°C (Figure 6A). Intriguingly, expression of the fusion protein restored telomere clustering in S-phase cells at 37°C in *ebp2-14* (Figure 6B), although the fusion protein did not suppress temperature-sensitive growth nor the defect in 60S ribosomal subunit biogenesis (Figure 6C and D). As a control, we expressed wild-type Ebp2, which suppressed both these latter defects (Figure 6C and D). The ability of the tethered fusion protein to suppress defects in telomere clustering but not the ribosome biogenesis separates the two functions ascribed to Ebp2. We conclude that the membrane-bound fraction of Ebp2 is indeed implicated in telomere clustering and telomeric repression, independent of its role in ribosome biogenesis.

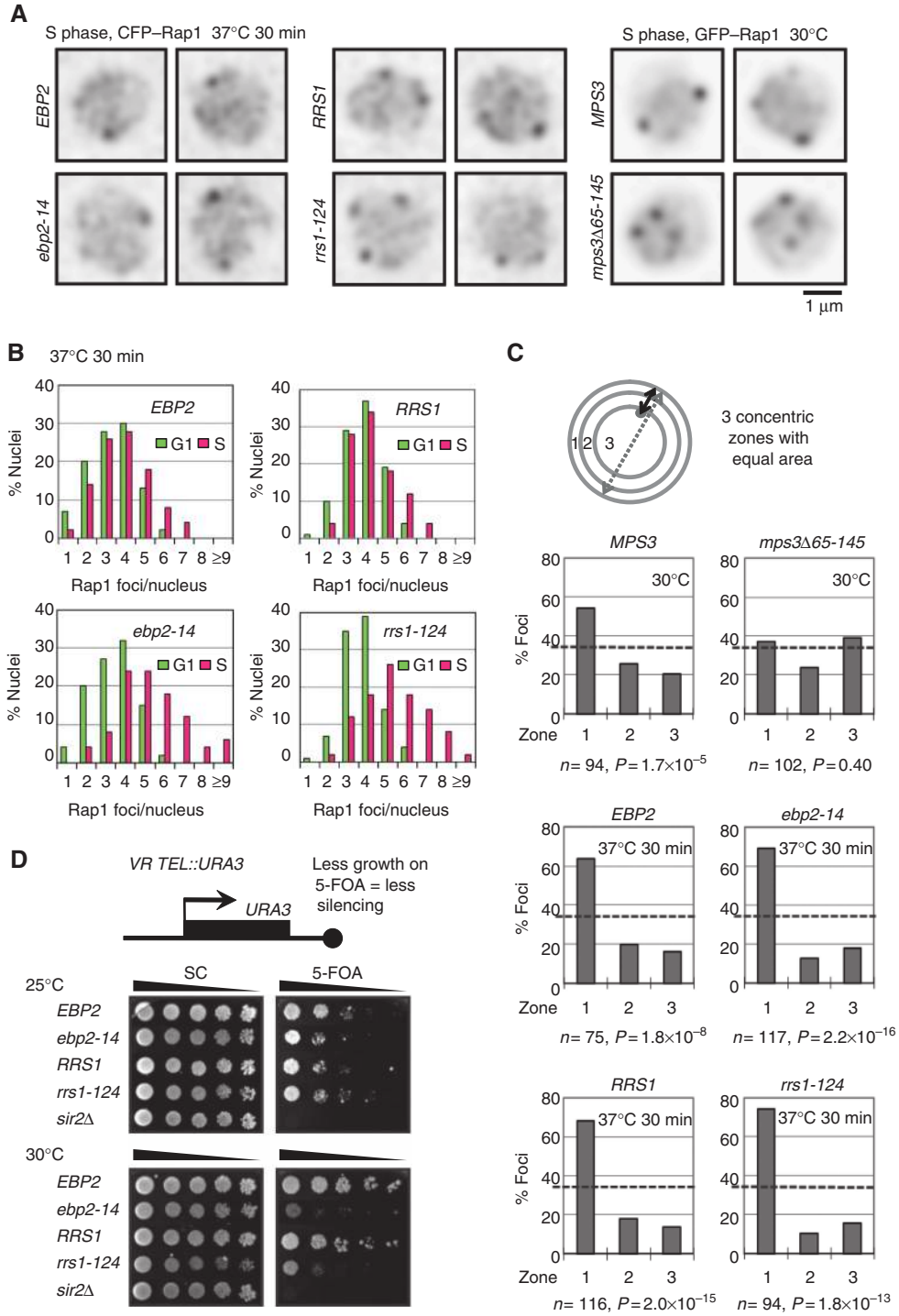


**Figure 5** Ebp2 and Rrs1 are required for telomere clustering and silencing, but not for telomere tethering. (**A**–**C**) *EBP2* (KM1128), *ebp2-14* (KM1129), *RRS1* (KM1130) and *rrs1-124* (KM1132) were grown asynchronously at 25°C and shifted to 37°C for 30 min. *MPS3* (GA6654) and *mps3Δ65-145* (GA6655) were grown asynchronously at 30°C. Representative images of CFP/GFP–Rap1 foci are shown in (**A**). The number of telomere foci marked by CFP/GFP–Rap1 in a 100 unbudded (G1 phase) and 50 small-budded (S phase) cells (ratio of the long axis length in daughter cell to that in the mother cell is $<1/3$) was counted in (**B**). The following are *P*-values that were calculated using the Mann–Whitney rank sum test. *EBP2* G1 phase: *ebp2-14* G1 phase $=0.51$ ($n=100$), *EBP2* S phase: *ebp2-14* S phase $=5.5\times10^{-5}$ ($n=50$), *RRS1* G1 phase: *rrs1-124* G1 phase $=0.66$ ($n=100$), *RRS1* S phase: *rrs1-124* S phase $=4.3\times10^{-4}$ ($n=50$). The distribution of telomere foci marked by CFP/GFP–Rap1 in zones 1, 2 and 3 is indicated in (**C**). CFP/GFP–Rap1 produces uniform low-intensity fluorescence throughout the yeast nucleoplasm, including the nucleolus. This background allows a precise determination of the nuclear periphery. The dotted line at 33% corresponds to a random distribution. Confidence values (*P*) for the $\chi^2$-test were calculated for each data set between random and test distributions. The number of cells examined in each data set is indicated (*n*). (**D**) Telomere silencing was analysed with the *URA3* reporter gene inserted at telomere V-R. The growth of five-fold serial dilutions of wild-type (*EBP2*: KM1149, *RRS1*: KM1153) and the *ebp2-14* (KM1152), *rrs1-124* (KM1155) and *sir2*Δ (YG881) strain cells on the medium containing 0.6 g/l 5-FOA at 25 and 30°C shows the repression level at telomere V-R. Representative colonies from three single colonies are shown.

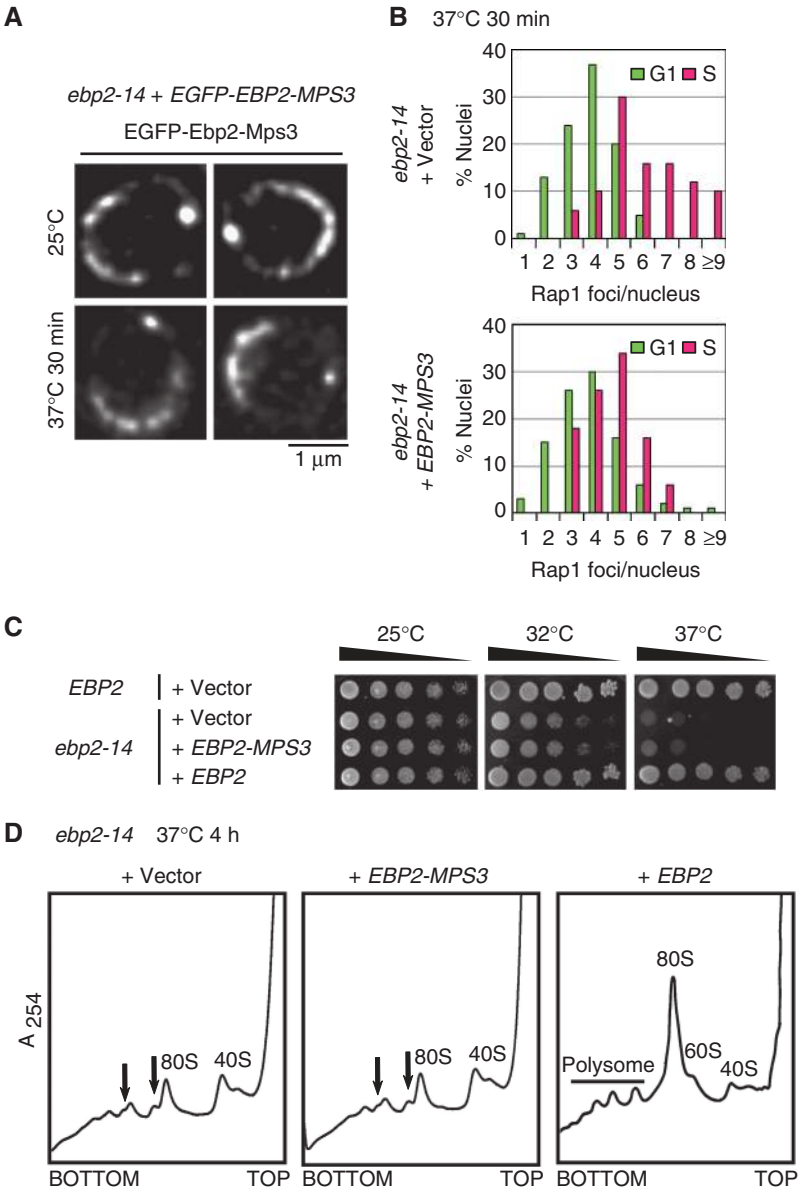


**Figure 6** Expression of Ebp2–Mps3 fusion proteins in *ebp2-14* suppresses a defect in telomere clustering but not defects in growth and ribosome biogenesis. (**A**) EGFP–Ebp2–Mps3 was expressed in *ebp2-14* (KM1290) and the localization was analysed at 25 and 37°C. (**B**) The *ebp2-14* cells with a plasmid expressing EGFP–Ebp2–Mps3 (KM1293) or a vector (KM1294) were grown asynchronously at 25°C and shifted to 37°C for 30 min. The number of telomere foci marked by CFP–Rap1 in a 100 unbudded (G1 phase) and 50 small-budded (S phase: ratio of the long axis length in daughter cell to that in the mother cell is $<1/3$) cells was counted. The following are *P*-values that were calculated using the Mann–Whitney rank sum test. Vector G1 phase: Fusion G1 phase = 0.63 ($n = 100$), Vector S phase: Fusion S phase = $6.3 \times 10^{-5}$ ($n = 50$). (**C**) $1 \times 10^7$ cells/ml and five-fold serial dilutions of cultures of *ebp2-14* cells with a plasmid expressing EGFP–Ebp2–Mps3 (KM1290), wild-type Ebp2 (KM1291), or a vector plasmid (KM1292) and *EBP2* cells with a vector plasmid (KM1289) were spotted on SC–His medium. (**D**) Polysome profiles in the *ebp2-14* mutant. The *ebp2-14* cells with a plasmid expressing EGFP–Ebp2–Mps3 (KM1290), wild-type Ebp2 (KM1292) or a vector plasmid (KM1291) were cultured at 37°C for 4 h, and free ribosomal subunits and polysomes in cell extracts were separated. Arrows indicate half-mer polysomes.

## Discussion

The data presented here demonstrated that Ebp2 and Rrs1 have at least two functions in budding yeast (Figure 7). First, as we previously reported, these proteins localize to the nucleolus, a prominent subnuclear compartment in which ribosomes are assembled. Both the downregulation and the mutation of these proteins can impair maturation of 25S rRNA and assembly of the 60S ribosomal subunit. Surprisingly, Ebp2 and Rrs1 are also found at the nuclear periphery where they interact with the SUN protein Mps3. We provide evidence that Ebp2 and Rrs1 also interact with Sir4, a component of silent chromatin domains at telomeres and contribute to the clustering of telomeres at the nuclear envelope.

As Ebp2 and Rrs1 have essential functions of ribosome biogenesis, we considered the possibility that the phenotypes of the *ebp2-14* and *rrs1-124* mutants in telomere maintenance might be the indirect result of a defect in ribosome synthesis. We can exclude this hypothesis based on the following

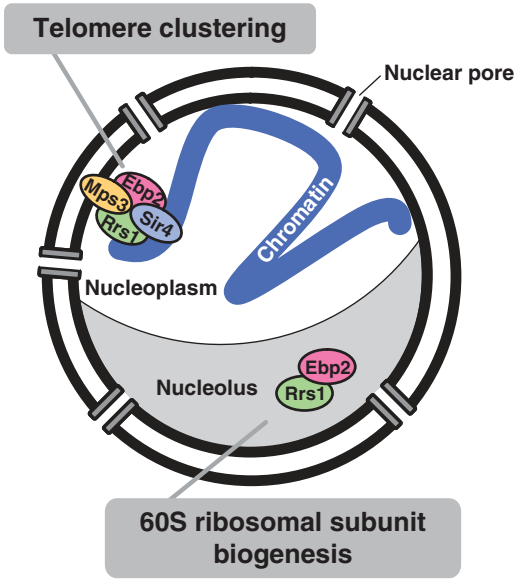


**Figure 7** A schematic model of the roles of Ebp2 and Rrs1 in the nucleus. Ebp2 and Rrs1 interact with each other and have an essential function in biogenesis of the 60S ribosomal subunit in the nucleolus. These proteins localize to the perinuclear region through Mps3, a SUN protein, and thereby serve a structural function in the mitotic nucleus. Ebp2, Rrs1 and Mps3 are associated with the silent information factor Sir4, and function in telomere clustering at the nuclear envelope.

results. First, the defect in telomere clustering occurs as early as 30 min after shifting *ebp2-14* or *rrs1-124* to restrictive temperature, whereas the defects in ribosome biogenesis are manifest 2 h later. Second, the expression of the Ebp2–Mps3 fusion protein in *ebp2-14* suppresses the defect in telomere clustering, but not the defect in ribosome biogenesis, arguing that the functions are separable.

### *Localization of Ebp2 and Rrs1 to the nuclear periphery*

Telomeres are maintained in clusters at the nuclear periphery in yeast through at least two redundant anchoring pathways that involve Sir4 and yKu. Both anchor at least partially through the transmembrane protein Mps3, at least in S-phase cells (Bupp *et al*, 2007; Schober *et al*, 2009). Our data suggest that Ebp2 and Rrs1 have a role in the maintenance of telomere clustering in S phase as well, supporting the notion that they cooperate with Mps3 and Sir4 to organize mitotic telomeres. We suggest that Mps3 anchors Ebp2 and Rrs1 at the nuclear periphery because both Ebp2 and Rrs1 are able to interact with Mps3 directly, and ectopic expression of the Mps3 N-terminus caused a delocalization of Ebp2 and Rrs1 from nuclear envelope.

We note that Ebp2 possesses three coiled-coil domains and can form homodimers (Figure 4B; Tsujii *et al*, 2000; Horigome *et al*, 2008), much like the C-terminus of Sir4. (Hattier *et al*, 2007). Given that the *ebp2* and *rrs1* mutations phenocopy the ectopic expression of the Mps3 N-terminus for maintenance of a spherical nuclear shape, we suggest that Ebp2 and Rrs1 are members of the perinuclear protein network of coiled-coil proteins that contributes to nuclear shape. Sir4, on the other hand, contributes to silencing and telomere position, but not nuclear shape.

### *Functions of Ebp2 and Rrs1 in telomere organization*

We are able to separate telomere clustering from telomere tethering by comparing phenotypes of the *ebp2-14*, *rrs1-124* and *mps3Δ65-145* mutants. All three mutants have increased numbers of Rap1 foci in S-phase cells, indicating that telomere clustering is compromised in each case. In contrast, telomeres remained localized to the nuclear envelope in the *ebp2-14* and *rrs1-124* strains, in contrast to the delocalization observed in *mps3Δ65-145*. It was reported that telomere clustering and SIR protein sequestration promote the repression of subtelomeric genes, whereas telomere tethering alone does not necessarily correlate with silencing (Mondoux *et al*, 2007; Taddei *et al*, 2009). Consistent with these reports, we observe that Ebp2 and Rrs1 have a function in telomere silencing, as does Mps3 (Bupp *et al*, 2007). Given that *ebp2-14* and *rrs1-124* defects in telomere clustering and silencing are manifest even in the presence of Mps3, we argue that Ebp2 and Rrs1 have crucial roles in silent domain organization at the nuclear periphery.

### *Linkage between ribosome biogenesis and telomere organization*

Since growing yeast cells dedicate a large amount of energy to ribosome biosynthesis, which includes ~80% of total transcription (reviewed by Warner, 1999), it is not surprising to find that it is regulated in response to environmental changes. Furthermore, it appears that ribosome biogenesis is linked to the cell cycle, cell size control and stress response (reviewed by Dez and Tollervey, 2004 and Jorgensen and Tyers, 2004). Although it would not be surprising to find that ribosome biogenesis is also connected with the nuclear organization, our study shows that we can dissociate the defects in telomere organization from the defects in ribosome biogenesis for Ebp2 and Rrs1, even though both proteins are clearly implicated in both events.

The bi-functionality of Ebp2 and Rrs1 nonetheless leaves open the possibility that the cell uses these proteins to coordinate ribosome biogenesis and telomere maintenance. Intriguingly, Rap1, the TG-repeat binding protein and Tbf1, a TTAGGG-recognizing protein that binds subtelomeric regions, function as transcriptional regulators of ribosomal protein genes or genes for snoRNAs, which have a key role in ribosome biogenesis (Preti *et al*, 2010). In addition, Tbf1 is the key protein necessary for transcription of ribosomal protein genes in *Candida albicans* (Hogues *et al*, 2008). It is possible that during evolution Tbf1 was replaced by Rap1 as a transcriptional factor for ribosomal protein genes (Hogues *et al*, 2008; Lavoie *et al*, 2010). Thus, even though we can show that the telomere defects of Ebp2 and Rrs1 are separable from ribosome biogenesis, this latter may be linked to telomere maintenance both on the transcriptional level and at the assembly stage.

### *Functions of mammalian orthologues of Ebp2 and Rrs1*

The homologues of Ebp2 and Rrs1 are relevant to various cellular responses in higher eukaryotes, such as Huntington's disease (Fossale *et al*, 2002), influenza virus replication (Geiss *et al*, 2001), response to fibroblast growth factor 3 (Reimers *et al*, 2001) and p53-dependent cell proliferation (Machida *et al*, 2006). The human orthologue, EBP2, has been identified in nucleoli purified from *HeLa* cells (Scherl *et al*, 2002), and co-fractionates with 28S rRNA in *HeLa* cells,

 

suggesting a role in ribosome biogenesis (Romanova *et al*, 2009). It is also localized to condensed chromosomes in mitosis (Kapoor and Frappier, 2003) and helps mediate the mitotic segregation of Epstein-Barr virus DNA episomes, which bind to mitotic chromosomes (Kapoor and Frappier, 2003). A recent study suggested that human RRS1, which also localizes to the nucleolus during interphase, is distributed at the chromosome periphery during mitosis and contributes to chromosome congression (Gambe *et al*, 2009). While preliminary, these results suggest that human EBP2 and RRS1 may also have multiple functions related to those described here for yeast. Further analysis of Ebp2 and Rrs1 and a deeper understanding of their function in nuclear organization may reveal features conserved among eukaryotes and shed light on the involvement of the human homologues in human diseases, such as those ascribed to the nuclear lamina.

## Materials and methods

### *Plasmids, strains and yeast methods*

Plasmids are listed in Supplementary Table S1. All yeast strains are derivatives of W303 (*his3-11, 15 ade2-1 ura3-1 leu2-3,112 trp1-1 can1-100*) and listed in Supplementary Table S2. Standard techniques were used for DNA and yeast manipulations. Yeast cells were grown in synthetic complete medium containing 2% glucose (SC) or SC dropout medium. To test the telomere clustering, *CFP–RAP1* fusion was integrated into the genome as follows: a 2.9-kb *RAP1* fragment that lack the 5′ end of the gene was PCR amplified using primers, 5′-AAAGCTAGCTCCGAGTATGGTCGTTGTTGA-3′ and 5′-AAACAGCTGCCTCCACAGAAAGTTCTTTATC-3′, and inserted into pRS306 digested with *Xba*I–*Sma*I after digestion with *Nhe*I–*Pvu*II. *CFP* was PCR amplified from pDH3 and inserted into the *Nru*I site of *RAP1*. Haploid strains were transformed with the plasmid after digestion with *Spe*I, which resides within a portion of the *RAP1* coding region at the 5′ side to the *CFP* gene. The resulting *CFP–RAP1* fusion construct contains the chromosomal *RAP1* gene intervened by the *CFP* gene under regulation of the authentic *RAP1* promoter. Similarly, in the wild-type and *mps3Δ65-145* strains, pAH52 was digested with *Pst*I which resides within a portion of the *RAP1* coding region at the 5′ side to the *GFP-S65T* gene (Hayashi *et al*, 1998). For the silencing assay, the strain CCFY100 (Roy and Runge, 2000) was transformed with a single copy plasmid pRS313 containing each of the *ebp2* and *rrs1* alleles and subsequently with the DNA fragment containing the *ebp2::LEU2* or *rrs1::LEU2* disruption, respectively. YG881 (*sir2*Δ; a gift from Dr D Shore) was used as a control strain.

### *Polysome and [methyl-$^3$H] methionine pulse-chase analyses*

Sucrose density gradient ultracentrifugation and [*methyl*-$^3$H] methionine pulse-chase analysis were carried out as described previously (Shirai *et al*, 2004; Yamada *et al*, 2007).

### *Protein–protein interactions*

GST pull-down and yeast two-hybrid assays of protein–protein interactions were performed as described previously (Shirai *et al*, 2004; Nariai *et al*, 2005). In yeast two-hybrid assays, interactions between the indicated fusion proteins were tested in yeast L40 strain with a *HIS3* reporter gene. A plasmid expressing lexA binding domain–Adh1 fusion protein was used as a negative control. 3-Amino-1,2,4-triazole (3-AT) was used as an inhibitor of the *HIS3* gene product. Immunoprecipitation using liquid nitrogen ground lysates was performed as described previously with minor modifications (Jaspersen *et al*, 2006). Ground cell powder was subjected to crosslinking with 0.2 mg/ml dithiobis (succinimidyl-propionate; Pierce Biotechnology) for 10 min. After the quenching reaction, lysates were sonicated in the extraction buffer containing 1 M NaCl and 1% Triton X-100. Lysates were centrifuged and the resulting supernatant was used for immunoprecipitation. Immunoprecipitation and washing the beads were performed in the following buffers: 100 mM/150 mM NaCl, 25 mM Hepes-KOH, pH 7.5, 0.1% Triton X-100, 2 mM EDTA, 2 mM $MgCl_2$, 1 mM DTT, 1 mM PMSF, and 1 μg/ml each of Pepstatin A, AEBSF, Bestatin and Leupeptin.

### *Microscopy*

Yeast cells grown to mid-log phase were harvested and spotted onto slides for immediate microscopic examination. Images for Figures 2A and 5B were acquired using Slide Book 4 Digital Microscopy software (Intelligent Imaging Innovations). Images on Figures 2B, C, 3C–E, 5A and C were acquired using a Metamorph-driven the Spinning-disk confocal system, and deconvolution was performed using the Huygens software (calculated PSF) and Imaris (Biplane) software for analysis of localization. The number of CFP/GFP–Rap1 foci was counted in typically 21–24 stacks of 0.2 μm. Telomere position was measured by ImageJ (NIH, USA) and the plug-in software PointPicker (Swiss Federal Institute of Technology Lausanne). All images were adjusted for background using Adobe Photoshop or Imaris.

### *Supplementary data*

Supplementary data are available at *The EMBO Journal* Online (http://www.embojournal.org).

## Acknowledgements

This paper is dedicated to the memory of our dear colleague, Takafumi Okada, whose promising life ended abruptly in April 2011. We are grateful to JR Warner (Albert Einstein College of Medicine) and JL Woolford, Jr (Carnegie Mellon University) for valuable discussion; K Wang for technical assistance; D Shore (University of Geneva) for yeast strains and plasmids; S Nishikawa (Nagoya University) and Yeast Resource Center for plasmids. This research was in part supported by grants from JSPS and the MEXT of Japan to KM. CH was supported by a JSPS Research Fellowship for Young Scientists. CH and SMG thank the Novartis Research Foundation and the Swiss National Science foundation NCCR 'Frontiers in Genetics' for support.

*Author contributions*: CH, TO and KS performed the experiments. CH, SMG and KM designed and analysed the experiments and wrote the article.

## Conflict of interest

The authors declare that they have no conflict of interest.

## References

Andersen JS, Lyon CE, Fox AH, Leung AK, Lam YW, Steen H, Mann M, Lamond AI (2002) Directed proteomic analysis of the human nucleolus. *Curr Biol* **12:** 1–11

Antoniacci LM, Kenna MA, Skibbens RV (2007) The nuclear envelope and spindle pole body-associated Mps3 protein bind telomere regulators and function in telomere clustering. *Cell Cycle* **6:** 75–79

Bupp JM, Martin AE, Stensrud ES, Jaspersen SL (2007) Telomere anchoring at the nuclear periphery requires the budding yeast Sad1-UNC-84 domain protein Mps3. *J Cell Biol* **179:** 845–854

Conrad MN, Lee CY, Chao G, Shinohara M, Kosaka H, Shinohara A, Conchello JA, Dresser ME (2008) Rapid telomere movement in meiotic prophase is promoted by NDJ1, MPS3, and CSM4 and is modulated by recombination. *Cell* **133:** 1175–1187

Conrad MN, Lee CY, Wilkerson JL, Dresser ME (2007) Mps3 mediates meiotic bouquet formation in *Saccharomyces cerevisiae*. *Proc Natl Acad Sci U S A* **104:** 8863–8868

Crisp M, Liu Q, Roux K, Rattner JB, Shanahan C, Burke B, Stahl PD, Hodzic D (2006) Coupling of the nucleus and cytoplasm: role of the LINC complex. *J Cell Biol* **172:** 41–53

Dez C, Tollervey D (2004) Ribosome synthesis meets the cell cycle. *Curr Opin Microbiol* **7:** 631–637

Doye V, Wepf R, Hurt EC (1994) A novel nuclear pore protein Nup133p with distinct roles in poly(A)+ RNA transport and nuclear pore distribution. *EMBO J* **13:** 6062–6075

Ebrahimi H, Donaldson AD (2008) Release of yeast telomeres from the nuclear periphery is triggered by replication and maintained by suppression of Ku-mediated anchoring. *Genes Dev* **22:** 3363–3374

Fossale E, Wheeler VC, Vrbanac V, Lebel LA, Teed A, Mysore JS, Gusella JF, MacDonald ME, Persichetti F (2002) Identification of a presymptomatic molecular phenotype in Hdh CAG knock-in mice. *Hum Mol Genet* **11:** 2233–2241

Gambe AE, Matsunaga S, Takata H, Ono-Maniwa R, Baba A, Uchiyama S, Fukui K (2009) Nucleolar protein RRS1 contributes to chromosome congression. *FEBS Lett* **583:** 1951–1956

Gartenberg MR, Neumann FR, Laroche T, Blaszczyk M, Gasser SM (2004) Sir-mediated repression can occur independently of chromosomal and subnuclear contexts. *Cell* **119:** 955–967

Gasser SM, Cockell MM (2001) The molecular biology of the SIR proteins. *Gene* **279:** 1–16

Geiss GK, An MC, Bumgarner RE, Hammersmark E, Cunningham D, Katze MG (2001) Global impact of influenza virus on cellular pathways is mediated by both replication-dependent and -independent events. *J Virol* **75:** 4321–4331

Gotta M, Laroche T, Formenton A, Maillet L, Scherthan H, Gasser SM (1996) The clustering of telomeres and colocalization with Rap1, Sir3, and Sir4 proteins in wild-type *Saccharomyces cerevisiae*. *J Cell Biol* **134:** 1349–1363

Gottschling DE, Aparicio OM, Billington BL, Zakian VA (1990) Position effect at S. cerevisiae telomeres: reversible repression of Pol II transcription. *Cell* **63:** 751–762

Hattier T, Andrulis ED, Tartakoff AM (2007) Immobility, inheritance and plasticity of shape of the yeast nucleus. *BMC Cell Biol* **8:** 47

Hayashi A, Ogawa H, Kohno K, Gasser SM, Hiraoka Y (1998) Meiotic behaviours of chromosomes and microtubules in budding yeast: relocalization of centromeres and telomeres during meiotic prophase. *Genes Cells* **3:** 587–601

Hediger F, Neumann FR, Van Houwe G, Dubrana K, Gasser SM (2002) Live imaging of telomeres: yKu and Sir proteins define redundant telomere-anchoring pathways in yeast. *Curr Biol* **12:** 2076–2089

Henras AK, Soudet J, Gérus M, Lebaron S, Caizergues-Ferrer M, Mougin A, Henry Y (2008) The post-transcriptional steps of eukaryotic ribosome biogenesis. *Cell Mol Life Sci* **65:** 2334–2359

Hogues H, Lavoie H, Sellam A, Mangos M, Roemer T, Purisima E, Nantel A, Whiteway M (2008) Transcription factor substitution during the evolution of fungal ribosome regulation. *Mol Cell* **29:** 552–562

Horigome C, Okada T, Matsuki K, Mizuta K (2008) A ribosome assembly factor Ebp2p, the yeast homologue of EBNA1-binding protein 2, is involved in the secretory response. *Biosci Biotechnol Biochem* **72:** 1080–1086

Hoskins J, Butler JS (2008) RNA-based 5-fluorouracil toxicity requires the pseudouridylation activity of Cbf5p. *Genetics* **179:** 323–330

Jaspersen SL, Giddings Jr TH, Winey M (2002) Mps3p is a novel component of the yeast spindle pole body that interacts with the yeast centrin homologue Cdc31p. *J Cell Biol* **159:** 945–956

Jaspersen SL, Martin AE, Glazko G, Giddings Jr TH, Morgan G, Mushegian A, Winey M (2006) The Sad1-UNC-84 homology domain in Mps3 interacts with Mps2 to connect the spindle pole body with the nuclear envelope. *J Cell Biol* **174:** 665–675

Jorgensen P, Tyers M (2004) How cells coordinate growth and division. *Curr Biol* **14:** R1014–R1027

Kapoor P, Frappier L (2003) EBNA1 partitions Epstein-Barr virus plasmids in yeast cells by attaching to human EBNA1-binding protein 2 on mitotic chromosomes. *J Virol* **77:** 6946–6956

Laroche T, Martin SG, Gotta M, Gorham HC, Pryde FE, Louis EJ, Gasser SM (1998) Mutation of yeast Ku genes disrupts the subnuclear organization of telomeres. *Curr Biol* **8:** 653–656

Laroche T, Martin SG, Tsai-Pflugfelder M, Gasser SM (2000) The dynamics of yeast telomeres and silencing proteins through the cell cycle. *J Struct Biol* **129:** 159–174

Lavoie H, Hogues H, Mallick J, Sellam A, Nantel A, Whiteway M (2010) Evolutionary tinkering with conserved components of a transcriptional regulatory network. *PLoS Biol* **8:** e1000329

Machida YJ, Chen Y, Machida Y, Malhotra A, Sarkar S, Dutta A (2006) Targeted comparative RNA interference analysis reveals differential requirement of genes essential for cell proliferation. *Mol Biol Cell* **17:** 4837–4845

Miele A, Bystricky K, Dekker J (2009) Yeast silent mating type loci form heterochromatic clusters through silencer protein-dependent long-range interactions. *PLoS Genet* **5:** e1000478

Miki F, Kurabayashi A, Tange Y, Okazaki K, Shimanuki M, Niwa O (2004) Two-hybrid search for proteins that interact with Sad1 and Kms1, two membrane-bound components of the spindle pole body in fission yeast. *Mol Gen Genomics* **270:** 449–461

Miyoshi K, Shirai C, Horigome C, Takenami K, Kawasaki J, Mizuta K (2004) Rrs1, a ribosomal protein L11-binding protein, is required for nuclear export of the 60S pre-ribosomal subunit in *Saccharomyces cerevisiae*. *FEBS Lett* **565:** 106–110

Mondoux MA, Scaife JG, Zakian VA (2007) Differential nuclear localization does not determine the silencing status of *Saccharomyces cerevisiae* telomeres. *Genetics* **177:** 2019–2029

Moss T (2004) At the crossroads of growth control; making ribosomal RNA. *Curr Opin Genet Dev* **14:** 210–217

Nariai M, Tanaka T, Okada T, Shirai C, Horigome C, Mizuta K (2005) Synergistic defect in 60S ribosomal subunit assembly caused by a mutation of Rrs1p, a ribosomal protein L11-binding protein, and 3′-extension of 5S rRNA in *Saccharomyces cerevisiae*. *Nucleic Acids Res* **33:** 4553–4562

Nishikawa S, Terazawa Y, Nakayama T, Hirata A, Makio T, Endo T (2003) Nep98p is a component of the yeast spindle pole body and essential for nuclear division and fusion. *J Biol Chem* **278:** 9938–9943

Preti M, Ribeyre C, Pascali C, Bosio MC, Cortelazzi B, Rougemont J, Guarnera E, Naef F, Shore D, Dieci G (2010) The telomere-binding protein Tbf1 demarcates snoRNA gene promoters in *Saccharomyces cerevisiae*. *Mol Cell* **38:** 614–620

Reimers K, Antoine M, Zapatka M, Blecken V, Dickson C, Kiefer P (2001) NoBP, a nuclear fibroblast growth factor 3 binding protein, is cell cycle regulated and promotes cell growth. *Mol Cell Biol* **21:** 4996–5007

Romanova L, Grand A, Zhang L, Rayner S, Katoku-Kikyo N, Kellner S, Kikyo N (2009) Critical role of nucleostemin in pre-rRNA processing. *J Biol Chem* **284:** 4968–4977

Roy N, Runge KW (2000) Two paralogs involved in transcriptional silencing that antagonistically control yeast life span. *Curr Biol* **10:** 111–114

Scherl A, Couté Y, Déon C, Callé A, Kindbeiter K, Sanchez JC, Greco A, Hochstrasser D, Diaz JJ (2002) Functional proteomic analysis of human nucleolus. *Mol Biol Cell* **13:** 4100–4109

Schober H, Ferreira H, Kalck V, Gehlen LR, Gasser SM (2009) Yeast telomerase and the SUN domain protein Mps3 anchor telomeres and repress subtelomeric recombination. *Genes Dev* **23:** 928–938

Shirai C, Takai T, Nariai M, Horigome C, Mizuta K (2004) Ebp2p, the yeast homolog of Epstein-Barr virus nuclear antigen 1-binding protein 2, interacts with factors of both the 60 S and the 40 S ribosomal subunit assembly. *J Biol Chem* **279:** 25353–25358

Shore D (1994) RAP1: a protean regulator in yeast. *Trends Genet* **10:** 408–412

Taddei A, Hediger F, Neumann FR, Bauer C, Gasser SM (2004) Separation of silencing from perinuclear anchoring functions in yeast Ku80, Sir4 and Esc1 proteins. *EMBO J* **23:** 1301–1312

Taddei A, Van Houwe G, Nagai S, Erb I, van Nimwegen E, Gasser SM (2009) The functional importance of telomere clustering: global changes in gene expression result from SIR factor dispersion. *Genome Res* **19:** 611–625

Towbin BD, Meister P, Gasser SM (2009) The nuclear envelope - a scaffold for silencing? *Curr Opin Genet Dev* **19:** 180–186

Tschochner H, Hurt E (2003) Pre-ribosomes on the road from the nucleolus to the cytoplasm. *Trends Cell Biol* **13:** 255–263

 

Tsujii R, Miyoshi K, Tsuno A, Matsui Y, Toh-e A, Miyakawa T, Mizuta K (2000) Ebp2p, yeast homologue of a human protein that interacts with Epstein-Barr virus Nuclear Antigen 1, is required for pre-rRNA processing and ribosomal subunit assembly. *Genes Cells* **5:** 543–553

Tsuno A, Miyoshi K, Tsujii R, Miyakawa T, Mizuta K (2000) *RRS1*, a conserved essential gene, encodes a novel regulatory protein required for ribosome biogenesis in *Saccharomyces cerevisiae*. *Mol Cell Biol* **20:** 2066–2074

Tzur YB, Wilson KL, Gruenbaum Y (2006) SUN-domain proteins: 'Velcro' that links the nucleoskeleton to the cytoskeleton. *Nat Rev Mol Cell Biol* **7:** 782–788

Warner JR (1999) The economics of ribosome biosynthesis in yeast. *Trends Biochem Sci* **24:** 437–440

Yamada H, Horigome C, Okada T, Shirai C, Mizuta K (2007) Yeast Rrp14p is a nucleolar protein involved in both ribosome biogenesis and cell polarity. *RNA* **13:** 1977–1987